Defect Printability and Inspectability of Cr-less Phase-Shift Masks for the 70nm Node

J. Heumann[a], J. Schramm[a], KT Park[a*], T. Witte[a], A. Birnstein[a],
N. Morgana[b], M. Hennig[b], R. Pforr[b], J. Thiele[b], N. Schmidt[c], C. Aquino[c]

[a] - Advanced Mask Technology Center, Rähnitzer Allee 9, 01109 Dresden, Germany
[b] - Infineon Technologies AG, Königsbrücker Str. 180, 01099 Dresden, Germany
[c] - KLA-Tencor Corporation, 160 Rio Robles, San Jose, CA 95134-1809, USA
[*] - DPI assignee at AMTC

ABSTRACT

A chrome-less phase-shift mask for the 70nm technology was designed and manufactured. The mask contains "lines and spaces" including programmed defects. Each defect was characterized with respect to the critical dimension (CD) variation on wafer, defect size, aerial image deviation, as well as inspection capture rate. It was found that defects with an AIMS intensity deviation of above 9 % are to be considered critical. The corresponding critical defect size is dependent on the defect type. All lithographically significant mask defects were found reliably using a KLA 576 inspection tool.

Keywords: RET, chrome-less, phase-shift, defect printability, mask inspection, aerial imaging

INTRODUCTION

Defect printability studies are essential for the production of lithographically "defect-free" masks. In the mask shop aerial imaging microscopy is widely used for dispositioning and qualification of mask defects. Whether a mask defect is lithographically significant or not, can only be determined through a correlation of wafer and aerial image results performed for various process relevant defects. Tuning the inspection tool such that only lithographically significant defects are found and consequently repaired, the mask production yield can be improved considerably.

Resolution Enhancement Techniques (RET) play an increasing role as 193nm optical lithography is being extended to 70nm technologies and beyond. Chrome-less Phase Shifting is a promising RET, because the mask features exhibit a high optical contrast at the wafer level and a small mask error enhancement factor (MEEF)[1,2,3]. The manufacturing of Cr-less phase-shift masks (Cr-less PSM) has matured such that features for a 70nm technology can be resolved on the mask. The manufacturability and printability of Cr-less features is a prerequisite for the execution of a defect printability study.

In this paper the defect printability and inspectability of a mesa-style double-edge (de) Cr-less PSM for the 70nm technology node was studied. A "lines and spaces" pattern with an aspect ratio of 1:1 on wafer level was chosen, as this pattern has exhibited the highest defect printability in previous studies[4].

EXPERIMENTAL

At first a printability study of de Cr-less PSM features for varying mesa width was performed. For a mask pattern pitch of 600 nm and a mesa width of 130 nm a "lines and spaces" pattern with a 1:1 aspect ratio on wafer was achieved. Using these parameters the background pattern was generated, into which a variety of process relevant defects were programmed (see Fig. 1 and Tab. 1).

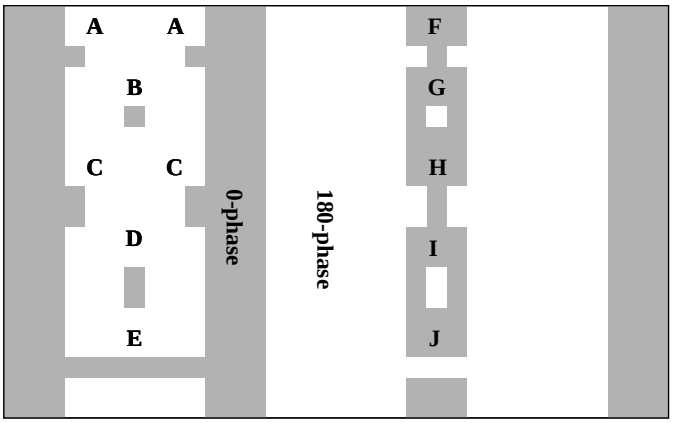

Fig. 1: Layout of programmed defects for a mesa-style de Cr-less PSM

In Fig. 1 gray areas correspond to non-etched quartz, whereas white areas correspond to etched quartz. The colors (gray and white) were chosen to correspond to the intensities in the aerial image. The programmed defects consist of extensions (quartz bump at a mesa feature, A & C), intrusions (quartz divot at a mesa feature, F & H), mesa bridges (quartz bump in an etched quartz area connecting two mesa features, E), mesa breaks (quartz divot intersecting a non-etched mesa feature, J), pin dots (quartz bump in a quartz-etched area, B & D), as well as pinholes (quartz divot in a non-etched quartz area, G & I). The extensions, intrusions, pin dots, and pinholes were designed with lateral aspect ratios of 1:1 (A, B, F, G) as well as 1:2 (C, D, H, I). Defect types A-E fall into the defect class "quartz bump", whereas defect types F-J can also be described as a quartz divot. All defect types mentioned above (see also Tab. 1) were designed in varying defect sizes.

	Defect type	**Defect class**
A	Extension with a 1:1 aspect ratio (left & right edge)	quartz bump
B	Pin dot with a 1:1 aspect ratio	
C	Extension with a 1:2 aspect ratio (left & right edge)	
D	Pin dot with a 1:2 aspect ratio	
E	Line bridge	
F	Intrusion with a 1:1 aspect ratio (left & right edge)	quartz divot
G	Pin hole defect with a 1:1 aspect ratio	
H	Intrusion with a 1:1 aspect ratio (left & right edge)	
I	Pin hole defect with a 1:2 aspect ratio	
J	Line break	

Tab. 1: List of programmed defect types implemented into the mesa-style de Cr-less PSM design

After finalizing the Cr-less PSM design a printability mask was manufactured. Each of the programmed defects was characterized with respect to wafer CD variation, defect size, and aerial image deviation using a Hitachi wafer Scanning Electron Microscope (SEM), a JEOL mask SEM, and a 193nm Aerial Image Microscope System (AIMS), respectively. Additionally the mask was used to evaluate the performance of a KLA 576 inspection system.

The SEM images of the programmed mask defects were often very different from the design image. The actual size and shape of a programmed defect was largely determined by mask process effects such as data biasing and corner rounding. Defects, whose actual shape was very different to the design intend (e.g. programmed extension, which resulted in a line bridge) were omitted in the evaluation. For the resultant plots only the lateral defect size measured from the SEM image was used.

The lateral defect size was determined using a image processing software. First the defect image was enhanced subtracting the pattern background. Second the defect circumference was plotted with a polygon and the inside area measured. The lateral defect sizes are given as the "square root of the area" (SRA). This method was chosen as in a previous study it had proved to correlated very well with the AIMS measurement values[4].

AIMS images were taken at best focus using an NA of 0,85 and a so-called disar aperature with a sigma of 0.9. The AIMS images were evaluated plotting a intensity profile through the defect, which was orientated vertical to the "lines

and spaces" pattern. First a defect-free area was identified as reference, for which the intensity maximum and minimum ($I_{ref,max}$ and $I_{ref,min}$) were determined. Second the "lines and spaces" area most effected by the defect was identified, and again the intensity maximum and minimum ($I_{def,max}$ and $I_{def,min}$) were determined. From these values the relative intensity deviations $(I_{def,max} - I_{ref,max})/(I_{ref\ max} - I_{ref,min})$ and $(I_{def,min} - I_{ref,min})/(I_{ref,max} - I_{ref,min})$ were calculated. The larger of the two absolute values determined the so-called AIMS intensity deviation.
The evaluation of the wafer SEM images was limited by the line-edge-roughness of the wafer patterns. A severity scoring was used, which groups the CD variations into different categories (see Tab. 2).

Severity score	CD Variation
0	None visible
1	Very slight
2	Slight
3	Medium
4	Medium-Large
5	Large
6	Bridge between lines Line break

Tab. 2: Wafer CD-variation severity scoring used

Integer values ranging from 0 to 6 were used for the scoring. An increasing number expresses an increasing CD-variation. "0" was used for no visible CD-variation, whereas line bridges and breaks were categorized as "6".
The defect inspection was performed using a variety of sensitivity settings. For each sensitivity setting 10 consecutive runs were performed. For each programmed defect the statistical capture rate was calculated.

RESULTS & DISCUSSION

For each programmed defect three characteristic values (defect size, AIMS intensity deviation, and wafer severity) were determined and plotted with respect to each other.

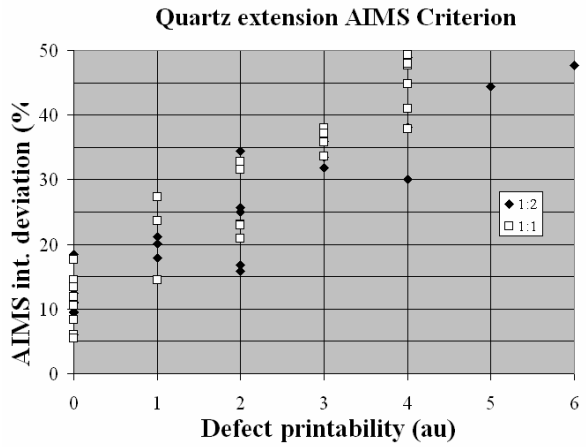

Fig. 2: AIMS intensity deviation plotted with respect to their defect printability
of extensions with a 1:1 and 1:2 aspect ratio.

Fig. 2 shows the AIMS intensity deviation (<50 %) plotted against the defect printability of extensions. There exists a considerable overlap of the individual severity categories, which is mainly attributed to the line-edge roughness seen in the wafer SEM images already mentioned. Within the margin of error no noticeable difference between extensions with a 1:1 and a 1:2 aspect ratio could be observed. The variety of programmed intrusions (not plotted) was very limited. The once available caused no visible wafer CD-variation (category "0"; measured AIMS intensity deviation < 10 %, see also Fig. 4, right image).

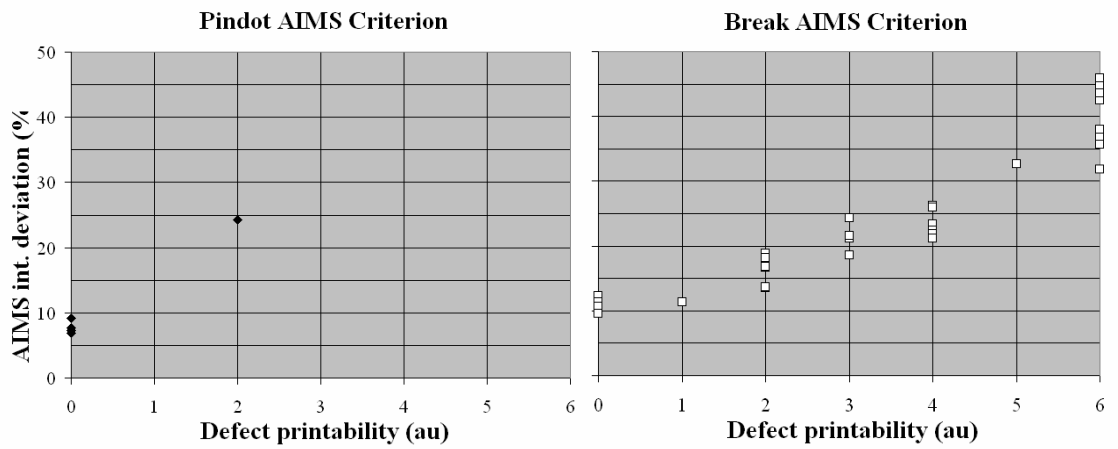

Fig. 3: AIMS intensity deviation plotted with respect to their defect printability of pin dots (left) and line breaks (right)

Fig. 3 has two graphs, in which again the AIMS intensity deviation is plotted against the defect printability of pin dots (left image) as well as line breaks (right image). The scaling of the axis is chosen identical to Fig. 2. For pin dots only four of the programmed defects were actually resolved. The line bridges (not plotted) all had an AIMS intensity deviation above 50 % and are therefore outside the area of interest. No data was available for pinholes, as the programmed defects were either not resolved or turned out as line breaks. For line breaks, similar to extensions, a large number of defects was present.

Within the margin of error quartz bumps (extensions and pin dots) exhibit a similar optical behavior. The slope of the "best-fit" line for quartz divots (only line breaks) is considerably less than for quartz bumps. The optically different behavior of the quartz bumps and divots with respect to the AIMS intensity deviation and the wafer CD-variation is still under investigation.

The AIMS criterion is the AIMS intensity deviation above which all defects are considered printing. Because of the large margin error a good correlation between the AIMS intensity deviation and the defect printability was not achieved. In order to minimize CD-variations on wafer all defects of category "1" (and above) are assumed to be critical for wafer manufacturing. Consequently all defects with an AIMS intensity deviation of > 11 % would need to be repaired.

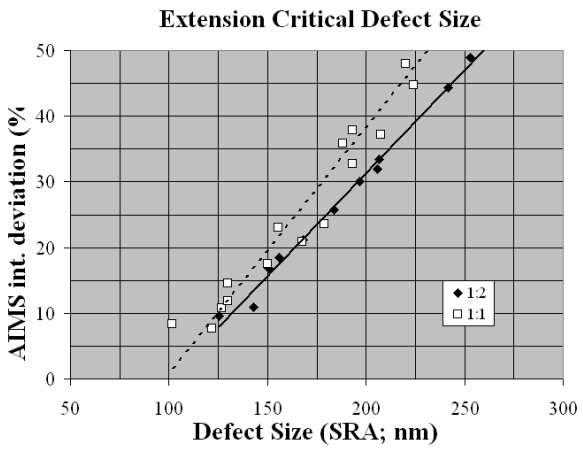

Fig. 4: AIMS intensity deviation with respect to the defect size of extensions with a 1:1 and a 1:2 aspect ratio

In Fig. 4 and Fig. 5 the AIMS intensity deviation was plotted against the defect size. The correlation of the plotted values is much better than in Fig. 2 and Fig. 3 indicating a much smaller margin of error for the mask than for the wafer related measurement values. For extensions (Fig. 4, left image) a difference between lateral aspect ratios of 1:1 and 1:2

is visible. Defects with a 1:1 aspect ratio consequently have a higher AIMS intensity deviation than defects with a 1:2 aspect ratio. Simulations performed for chrome defects using the Kirchhoff approximation didn't reflect this behavior. Simulations of quartz defects are currently being performed. Intrusions (not plotted) were only realized for defect sizes between 90 nm and 150 nm. The respective AIMS intensity deviations fluctuated between 4 % and 10 %, which is within the repeatability of the AIMS, showing no correlation to the defect size. Applying a AIMS criterion of 11 % the critical defect size of extensions with a lateral aspect ratio of 1:1 and 1:2 is approx. 125 nm and 130 nm, respectively.

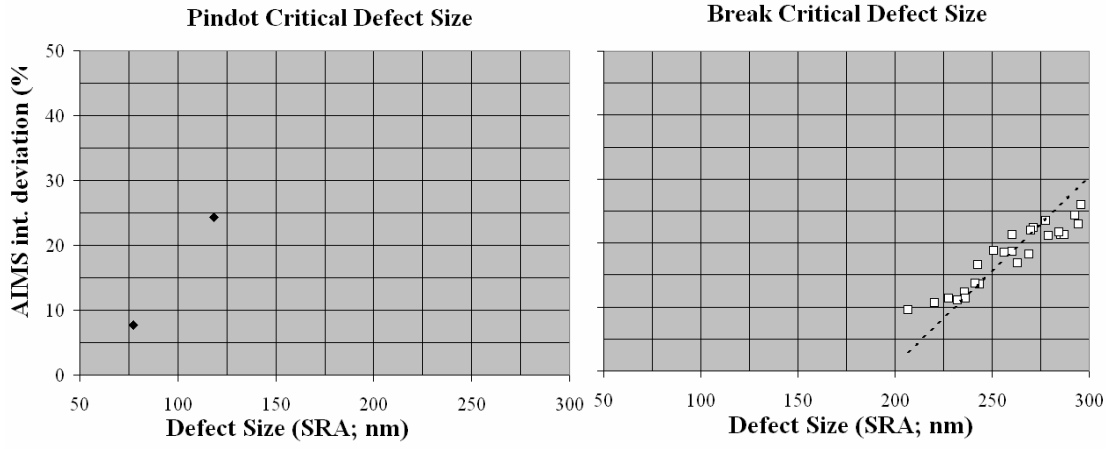

Fig. 5: AIMS intensity deviation with respect to the defect size
of pin dots and line bridges (left image) as well as line breaks (right image)

Fig. 5 has two graphs, in which again the AIMS intensity deviation is plotted against the defect size of pin dots (left image) and line breaks (right image). The scaling of the axis is chosen identical to Fig. 4. For pin dots only very limited data is available. All line bridge fell outside the area of interest (AIMS > 50 %). Quartz bumps (extensions and pin dots) within the margin of error don't fall onto the same line. E.g. pin dots indicate to have a higher AIMS impact than extensions. This behavior also has been experienced in a previous study for MoSi defects[5].
In this study quartz divots (line breaks) show a much smaller AIMS impact than quartz bumps (compare plots in Fig. 4 and Fig. 5). In a similar study for Cr-less PSM mask this difference has not been observed[6]. When plotting the defect size with respect to the defect printability (not shown here, but can be deduced from Fig. 2&3 and Fig. 4&5) this difference is not apparent. Quartz bumps and divots within the margin of error have a similar slope with a line offset of approx. 80 nm. The offset could be explained with the SEM sizing method, which due to the defect's edge behavior make quartz divots to appear smaller than quartz bumps. Under this assumption the difference experienced between quartz bumps and divots would be related to the AIMS values, which is currently being investigated. Again applying an AIMS criterion of 11 % the critical defect size for pin dots is approx. 90 nm, whereas line breaks can be as large as 230 nm.
Defect inspection was performed for various sensitivity settings. For a KLA 576 inspection system the pixels named P125, P125P (TeraPhase), P90, and P90P (TeraPhase) were tested. For all pixels the UCFddT35 algorithm was used and a focus offset of 800 nm was applied. Inspection settings suitable for production were found using a defect free area. For all pixels the algorithms sensitivity settings had to be decreased in order to avoid defects, which could not be traced on the mask and therefore are believed to be tool related (false defect). For each of the pixels the sensitivity settings were tuned until the false defect density was approx. 1/cm^2 (see Tab. 3). For P90 even at minimum sensitivity settings the false defect density was approx. 10/cm^2. Consequently no further tests were performed for this pixel.

Pixel	sensitivity settings	av. bump sensitivity	av. divot sensitivity
P125P	70-95	88,73	62,88
P125	90-100	86,74	58,98
P90P	60-80	84,94	56,02

Tab. 3: List of sensitivity settings for each pixel found to be suitable for production
and the respective defect sensitivity average

The printability mask was inspected with the pixels and sensitivity settings listed in Tab. 3. To easily compare the overall sensitivity of each inspection setting, the average capture rate over all programmed defects (resolved and not resolved) was calculated for quartz bumps and divots. The highest defect sensitivity was achieved for P125P, followed by P125 and P90P. The performance difference between P125P and P90P as well as the optimal sensitivity settings for P90 are currently under investigation. In the following graphs only the sensitivity of the highest performing pixel (P125P) is plotted.

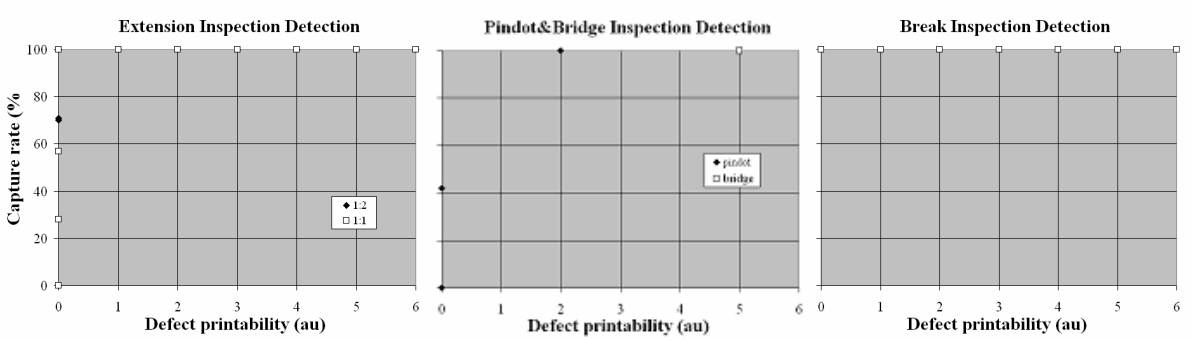

Fig. 6: Inspection capture rate with respect to the defect printability of extensions with a 1:1 and a 1:2 aspect ratio (left image), pin dots and line bridges (middle image), as well as line breaks (right image)

In Fig. 6 the inspection capture rate is plotted for extensions, pin dots, line bridges, and line breaks. All defects with wafer severity “1” and above have been found reliably. For extensions and pin dots some category “0” defects have been found with a capture rate below 100 %. Fine-tuning of the inspection tool such that only the lithographically significant defects are found was not possible, as desensing of the tool caused some category “1” extensions not to be found reliably, while still some category “0” breaks were still detected 100 %. As a consequence defect dispositioning using the AIMS tool is needed.

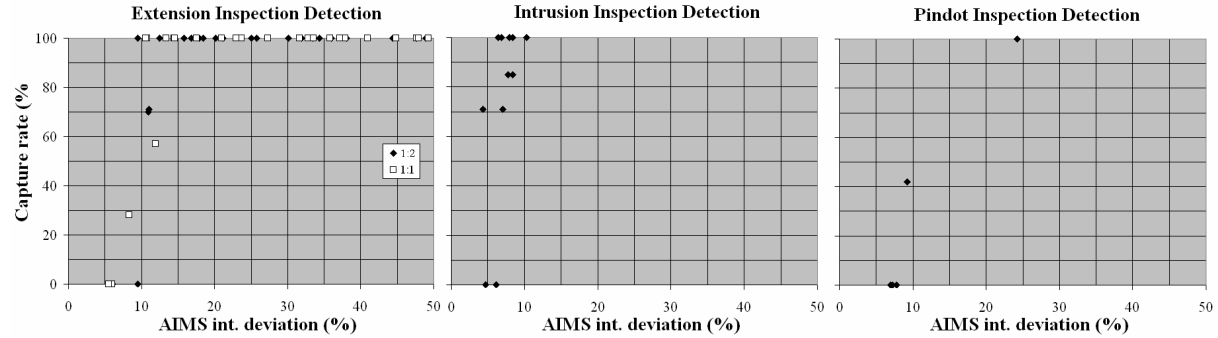

Fig. 7: Inspection capture rate with respect to the AIMS intensity deviation of extension with a 1:1 and 1:2 aspect ratio (left image), intrusions (middle image), as well as pin dots (right image)

In the mask shop AIMS is widely used for dispositioning of mask defects. In order to insure that all defects, which need repair, are found, it is important that all defects above the identified AIMS criteria (> 11 %) are found reliably. Fig. 7 displays the capture rate with respect to the AIMS intensity deviation of extensions (left image), intrusions (middle image), as well as pin dots (right image). For extensions the sensitivity roll-off occurs at AIMS intensity deviations below 12 %. For intrusions the capture rate is 100 % down to AIMS values of approx. 9 %. For pin dots only a few measurements points are available. The measurement point at an AIMS value of 9 % indicates that the sensitivity roll-off occurs in this region. No information about the sensitivity roll-off is available for line bridges and line breaks (not plotted). The smallest line bridge, which had an AIMS value of approx. 56 %, has been found reliably. Line breaks, which are available down to AIMS values of 7 %, also have been found reliably. Considering the AIMS margin of error of approx. 4 % all defects above the AIMS criteria were found reliably.

SUMMARY

For a mesa-style double-etch Cr-less PSM programmed defect mask the wafer CD variations and the AIMS intensity deviations exhibited a weak correlation. A large margin of error results from the line edge roughness on the wafer, which makes the measurement of the defect induced CD variation difficult. To improve the data correlation a so-called wafer severity scoring was introduced. It was found that defects with an AIMS intensity deviation of above 11 % are to be considered critical. The corresponding critical defect size is dependent on the defect type. Pin dots are critical above 90 nm. Extensions reaches a lithographically critical size at approx. 125 nm, whereas a line break can be as large as 230 nm. All lithographically significant mask defects were found reliably using the P125P-pixel of a KLA 576 inspection tool.

ACKNOWLEDGEMENTS

This work was supported by the German Federal Ministry of Education and Research (BMBF) under Contract No. 01M3154A.

REFERENCES

[1] J.F. Chen, *et. al*, „Binary Halftone Chromeless PSM Technology for λ/4 Optical Lithography", *Proceedings of SPIE*, Vol. 4346, pp. ,515-533SPIE, 2001

[2] Hsu, *et. al*, "Patterning Submicron DRAM Cell by Using Chromeless Phase Lithography", *Proceedings of SPIE*, Vol. 4691, pp. 76-88, SPIE, 2002

[3] Van Den Broeke, *et. al*, „Complex 2D Pattern Lithography at λ/4 Resolution Using Chromeless Phase Lithography (CPL)", *Proceedings of SPIE*, Vol. 4691, pp. 196-214, SPIE, 2002

[4] J. Heumann, M. Zarrabian, M. Hennig, W. Dettmann, L. Zurbrick, and M. Lang;" AltPSM Inspection Capability and Printability of Quartz Defects", *Proceedings of SPIE*, Vol. 4889, pp. 1033-1040, SPIE, 2002

[5] K. Eggers, K. Gutjahr, M. Peikert, D. Rutzinger, R. Ludwig, M. Kaiser, A. Dürr, and J. Heumann, "Defect Printability and Inspectability of Halftone Masks for the 90nm and 70nm Node", *GMM-Fachbericht*, Vol. 45, pp. 187-191, VDE Verlag, 2005

[6] Y. Marokawa, K. Kojima, H. Hashimoto, Y. Yoshida, S. Sasaki, H. Mohri, and N. Hayashi, "Defect Inspection and Repair Performance on CPL Masks for 90 and 65nm Node Line Patterns", *Proceedings of SPIE*, Vol. 5567, to be published, SPIE, 2005